J. Phys. A: Math. Gen. 27 (1994) 6091–6106. Printed in the UK

Semiclassical theory of magnetization for a two-dimensional non-interacting electron gas

S D Prado†, M A M de Aguiar†, J P Keating‡ and R Egydio de Carvalho§

† Instituto de Física Gleb Wataghin, Universidade Estadual de Campinas, Campinas 13083-970, São Paulo, Brazil

‡ Departament of Mathematics, University of Manchester, Manchester M13 9PL, UK

§ Instituto de Geociências e Ciências Exatas, Universidade Estadual Paulista, Rio Claro 13500-230, São Paulo, Brazil

Received 13 July 1993, in final form 11 July 1994

Abstract. We compute the semiclassical magnetization and susceptibility of non-interacting electrons, confined by a smooth two-dimensional potential and subjected to a uniform perpendicular magnetic field, in the general case when their classical motion is chaotic. It is demonstrated that the magnetization per particle $m(B)$ is directly related to the staircase function $N(E)$, which counts the single-particle levels up to energy E. Using Gutzwiller's trace formula for N, we derive a semiclassical expression for m. Our results show that the magnetization has a non-zero average, which arises from quantum corrections to the leading-order Weyl approximation to the mean staircase and which is independent of whether the classical motion is chaotic or not. Fluctuations about the average are due to classical periodic orbits and do represent a signature of chaos. This behaviour is confirmed by numerical computations for a specific system.

1. Introduction

Semiclassical theory shows that classical dynamics has an important influence on quantum energy spectra [1–3]. In the case of simple systems, such as the hydrogen atom in a strong magnetic field, the spectrum can be measured directly and put into correspondence with random-matrix statistical properties and with periodic orbit theory [4–7]. In more complex systems, however, a direct observation of the energy levels is usually not possible and so the effects of the underlying classical dynamics have to be studied in terms of other physical quantities.

The magnetic susceptibility of a system of charged particles was proposed by Nakamura and Thomas [8, 9] as one quantity whose quantum behaviour might depend sensitively on the chaotic nature of the associated classical motion. To understand why this is so, consider a system of $2P$ non-interacting electrons moving in a two-dimensional potential $V(x, y)$ and subject to a constant magnetic field B in the perpendicular direction. (Such systems have been used as models for small two-dimensional metallic particles where the free electrons only interact with the particle boundary, here represented by V.) At zero temperature the electrons fill the first P available levels (here we ignore the spin–field interaction). Now imagine changing the field strength B adiabatically, following the energy levels as functions of B. If the Hamiltonian is classically chaotic, no degeneracies are expected and the levels will fluctuate, exhibiting avoided crossings. If, on the other hand, it is integrable then the levels can (and typically do) cross, exhibiting a much smoother behaviour as B is varied.

0305-4470/94/186091+16$19.50

The magnetization m_0 and magnetic susceptibility χ_0 per electron at zero temperature are given as first and second-order derivatives of the total energy with respect to the field B, respectively,

$$m_0(B) = -\frac{1}{P}\sum_{n=1}^{P}\frac{\partial E_n}{\partial B}$$

$$\chi_0(B) = -\frac{1}{P}\sum_{n=1}^{P}\frac{\partial^2 E_n}{\partial B^2}.$$

At an avoided crossing between levels i and j at field strength B, both derivates $\partial^2 E_i/\partial B^2$ and $\partial^2 E_j/\partial B^2$ assume large values but have opposite signs and therefore their contributions nearly cancel. The contribution of the last filled level at an avoided crossing with the next (unfilled) level is, however, not cancelled, and this produces large peaks in $\chi_0(B)$. Moreover, it obviously follows that these peaks will correspond to enhanced susceptibility, because they are associated with maxima of the level curve. We should, of course, also remark that, as pointed out in [8], such peaks are not necessarily a signature of chaos. In fact, integrable or nearly integrable Hamiltonians present even sharper peaks than chaotic ones. Nevertheless, the dynamics of the energy levels as a function of the magnetic field is generally different for regular and chaotic systems, and the question is whether this leads to distinct behaviour in the susceptibility and magnetization.

In the work of Nakamura and Thomas [8] the systems considered were the circular billiard, which is integrable for all values of the applied magnetic field, and the elliptic billiard, which is integrable only for $B = 0$ [10]. The elliptic billiard in a magnetic field has also been used as a simple model to describe a rotating atomic nucleus, the susceptibility playing the role of the moment of inertia [11]. The diamagnetic properties of the spectrum in an elliptic shell have also been investigated in detail by Berman *et al* [12].

In this paper we study the semiclassical properties of $\chi(B)$ and $m(B)$ both theoretically and numerically. It will be shown that the magnetization can be expressed as a sum of a smooth term (its average) plus oscillatory contributions associated with classical periodic orbits. The smooth term is related to the corrections to Weyl's leading-order asymptotic approximation for the eigenvalue counting (staircase) function $N(E)$; the oscillatory terms are derived using Gutzwiller's trace formula [13]. At zero temperature all orbits contribute to $m_0(B)$, while for a finite temperature T only short orbits (with periods $\tau \leqslant \hbar/k_B T$) do so. A similar theory was recently constructed for billiard systems in [14]. This work goes beyond our study in that it considers Riemann–Siegel-type resummations [15, 16] of the divergent periodic orbit sums involved. However, it failed to include the Weyl-series terms, which turn out to play an important role in determining the magnetic properties.

The theory developed here shows that, contrary to the numerical conclusions drawn by Nakamura and Thomas [8], the magnitude of the susceptibility at zero magnetic field is, on average, *independent of whether the system is chaotic or not: it depends only on the Weyl* series for the mean of the staircase function and so is determined solely by global properties which are unrelated to the stability of the classical trajectories. This is confirmed by the results of our numerical tests.

For the numerical study we chose a smooth, non-integrable, non-scalable Hamiltonian which exhibits regular behaviour at low energies and chaotic behaviour at higher energies. By using different values of $\hbar$ we can choose the first P levels to lie completely in the regular region or mostly in the chaotic region. In this way (contrary to the study in [8]), all symmetry properties of the regular and chaotic cases are exactly the same (because they correspond to the same system) and hence any differences in the behaviour of $\chi(B)$ or

$m(B)$ can be attributed exclusively to the underlying classical dynamics. We also present results for the harmonic oscillator Hamiltonian [17], where the mean magnetization can be computed analytically and compared to the exact result.

The paper is organized as follows: in section 2 we derive the necessary semiclassical theory for the magnetization; in section 3 we show the results for the harmonic oscillator; in section 4 we define our smooth Hamiltonian and study its single-particle properties for various values of the magnetization field B, comparing the numerical results for $m(B)$ and $\chi(B)$ with the semiclassical theory of section 2; finally, section 5 is devoted to our conclusions.

2. Semiclassical theory of magnetization

2.1. Thermodynamics

The thermodynamic definition of the magnetization at temperature T is [18]

$$\mathcal{M}_T(B) = -\frac{\partial \mathcal{F}}{\partial B} \tag{1}$$

where

$$\mathcal{F} = -\frac{\partial}{\partial \beta} \log \mathcal{Z} \tag{2}$$

is the Helmholtz free energy, $\mathcal{Z}$ is the partition function, and $\beta = 1/k_B T$, where k_B is the Boltzmann constant. For a system of $2P$ non-interacting fermions at zero temperature, $\mathcal{F}$ is just the ground-state energy $2\sum_{n=1}^{P} E_n(B)$, where $E_n(B)$ are the single-particle energies, which depend on the magnetic field B. In this case, the magnetization per particle is simply

$$m_0(B) \equiv \frac{1}{2P}\mathcal{M}_0(B) = -\frac{1}{P}\sum_{n=1}^{P} \frac{\partial E_n}{\partial B}. \tag{3}$$

Finite temperatures may be taken into account by incorporating the Fermi function

$$g_T(E) = \frac{1}{1 + z^{-1}e^{\beta E}} \tag{4}$$

where z, the chemical potential, depends on the magnetic field and the temperature through the constraint

$$\sum_{n=1}^{\infty} \frac{1}{1 + z^{-1}e^{\beta E_n}} = P. \tag{5}$$

In terms of $g_T(E)$, the magnetization per particle at finite temperatures is given by

$$m_T(B) = -\frac{1}{P}\sum_{n=1}^{\infty} g_T(E_n)\frac{\partial E_n}{\partial B}. \tag{6}$$

Notice that, according to (4), as $T \to 0$ $g_T(E_n)$ approaches a step function centred at the Fermi energy $E_f = (1/\beta)\log z$, which satisfies $E_P \leqslant E_f < E_{P+1}$. Hence in this limit (6) reduces to (3).

We now show that both expressions (3) and (6) can be written in terms of the spectral staircase

$$N(E, B) = \sum_{n=1}^{\infty} \Theta(E - E_n(B)) \tag{7}$$

where Θ denotes the unit step function. For the case of zero temperature, it is trivial to see that

$$m_0(B) = \frac{1}{P}\int_0^{E_f} \frac{\partial N}{\partial B}\,dE\,. \tag{8}$$

For $T \neq 0$ we have from (6) that more generally

$$\begin{aligned} m_T(B) &= \frac{1}{P}\int_0^{\infty} g_T(E)\left(-\sum_n \frac{\partial E_n}{\partial B}\delta(E - E_n(B))\right)dE \\ &= \frac{1}{P}\int_0^{\infty} g_T(E)\frac{\partial N}{\partial B}(E, B)\,dE\,. \end{aligned} \tag{9}$$

As $T \to 0$ it is clear that (9) reduces to (8).

2.2. *Semiclassical limit*

Having expressed the magnetization in terms of the spectral staircase, it is a simple matter to take the semiclassical limit. Writing

$$N(E, B) \approx \overline{N} + N_{\text{osc}} \tag{10}$$

we can use the fact that, as $\hbar \to 0$, the average part may be represented in the form

$$\overline{N} = N_{\text{Weyl}} + \text{corrections} = \frac{1}{\hbar^2}\int \Theta(E - H(q, p))\,d^2q\,d^2p + \text{corrections} \tag{11}$$

where the correction terms constitute an asymptotic series in increasing powers of $\hbar$, and the oscillatory part is given by

$$N_{\text{osc}}(E, B) = \frac{1}{\pi}\sum_p \sum_{j=1}^{\infty} \frac{A_{p,j}}{j}\sin\left(\frac{jS_p}{\hbar} - \frac{\pi\sigma_{pj}}{2}\right) \tag{12}$$

with

$$A_{p,j}(E, B) = \frac{1}{\sqrt{\det(M_p^j - I)}} \tag{13}$$

where M, S and σ are the monodromy matrix, action and Maslov index of the primitive periodic orbits, labelled p, and their repetitions, labelled j [13].

We first consider the contributions from the average term $\overline{N}$. As discussed in Peierls [19], the Weyl term itself does not contribute to the magnetization for systems with a Hamiltonian of the form kinetic-plus-potential energy. This is because the change of variables

$$\Pi = p - \frac{e}{c}A(q) \qquad R = q$$

has unit Jacobian and removes any vector-potential dependence from the integral in (11). In other words N_{Weyl} is independent of B. Therefore, the (quantum mechanical) corrections to N_{Weyl} are very important and at least the dominant terms must be computed. We shall do this calculation explicitly for the harmonic oscillator in section 3 and for the Nelson potential in the appendix.

Proceeding with the oscillatory contributions, we write

$$m_T(B) \approx \overline{m}_T(B) + m_T^{\text{osc}}(B) \tag{14}$$

where $\overline{m}_T(B)$ is the average part coming from the corrections to N_{Weyl}. It follows from (4) and (9) that

$$m_T^{\text{osc}}(B) = \sum_p \sum_{j=1}^{\infty} \frac{1}{\pi\hbar P} \int_0^{\infty} \frac{1}{1+z^{-1}e^{\beta E}} a_{p,j} A_{p,j} \cos\left(\frac{jS_p}{\hbar} - \frac{\sigma_{p,j}\pi}{2}\right) dE \tag{15}$$

where

$$a_p = \frac{\partial S_p}{\partial B} \tag{16}$$

is the analogue of the primitive period $\partial S_p/\partial E$ appearing in the semiclassical density of states [13]. Assuming that $kT \ll E_f$, the integral in (15) can be evaluated in the semiclassical limit, giving

$$m_T^{\text{osc}}(B) \approx \frac{2kT}{P\hbar} \sum_p \sum_{j=1}^{\infty} A_{p,j} a_p \sin\left(\frac{jS_p}{\hbar} - \frac{\pi}{2} j\sigma_p\right) \frac{\exp\left(-\pi kT\tau_{pj}/\hbar\right)}{\left[1-\exp\left(-2\pi kT\tau_{pj}/\hbar\right)\right]} \tag{17}$$

where $A_{p,j}$, S_p, σ_p, and the period τ_p are evaluated at the Fermi energy $E = E_f$. It is clear from this expression that the contribution of each periodic orbit to m_T^{osc} consists of a sinusoidal oscillation of period $2\pi\hbar/ja_p$. Taking the limit as $T \to 0$ gives

$$m_0^{\text{osc}}(B) \approx \frac{1}{\pi P} \sum_p \sum_{j=1}^{\infty} \frac{A_{p,j} a_p}{j\tau_p} \sin\left(\frac{jS_p}{\hbar} - \frac{\pi}{2} j\sigma_p\right) \tag{18}$$

where again all quantities are evaluated at energy $E = E_f$.

In order to study the fluctuations in the magnetization, it is useful to compute the Fourier transform of m_T^{osc}. Since $m_T(B)$ is an odd function of B, this may be defined as

$$\tilde{m}_T^{\text{osc}}(a) = \int_0^{\infty} m_T^{\text{osc}}(B) \sin(aB/\hbar)\, dB\,. \tag{19}$$

For low temperatures we may substitute (17) for $m_T^{\text{osc}}(B)$ and so find in the semiclassical limit that if i labels the solutions of $ja_p(B_i) = a$ then

$$\tilde{m}_T^{\text{osc}}(a) = \frac{\pi kT}{P} \sum_p \sum_{j=1}^{\infty} \sum_i \frac{A_{p,j} a_p \exp\left(-\pi kT\tau_{pj}/\hbar\right)}{\left[1-\exp\left(-2\pi kT\tau_{pj}/\hbar\right)\right]} \times \cos\left(\frac{jS_p}{\hbar} - \frac{\pi}{2}\sigma_{pj}\right) \left\{\delta(ja_p - a) - \delta(ja_p + a)\right\} \tag{20}$$

which shows peaks at $a = ja_p(E_f)$ in analogy with the peaks at $\tau = j\partial S_p/\partial E$ of the Fourier transform of the density of states [2, 5, 20].

It may be seen from (17) that the effect of finite temperatures is to truncate the periodic orbit sum in period τ. To isolate contributions from small-a_p orbits it is necessary to smooth $m_T^{\text{osc}}(B)$ with respect to B. Hence we take the convolution of (17) with a Gaussian of width λ, that is, we define

$$m_{T,\lambda}^{\text{osc}}(B) \equiv \frac{1}{\lambda\sqrt{2\pi}} \int_{-\infty}^{\infty} m_T^{\text{osc}}(B') e^{-(B-B')^2/2\lambda^2}\, dB'\,. \tag{21}$$

For low temperatures, the semiclassical form of $m_{T,\lambda}^{\text{osc}}$ may be obtained by substituting the periodic orbit sum (17) into the integral, giving the result

$$m_{T,\lambda}^{\text{osc}}(B) \approx \frac{2kT}{\hbar P} \sum_{p,j} A_{p,j} a_p \frac{\exp\left(-\pi kT\tau_p j/\hbar\right)}{\left[1-\exp\left(-2\pi kT\tau_p j/\hbar\right)\right]} \times \sin\left(j\frac{S_p}{\hbar}(E_f, B) - \frac{\pi}{2} j\sigma_p\right) \exp\left(-\frac{\lambda^2 j^2 a_p^2(E_f, B)}{2\hbar^2}\right) \tag{22}$$

which clearly shows the desired truncation in a_p.

In conclusion, the power spectrum of $m^{\mathrm{osc}}_{T,\lambda}(B)$ gives peaks at $ja_p = j\partial S_p/\partial B$ and cuts off the contribution of long orbits if $T \neq 0$, and of large-a_p orbits if $\lambda \neq 0$. Equivalent expressions for the semiclassical susceptibility can be obtained directly by differentiating (17) and (18) with respect to B. Clearly this implies that oscillatory terms in $\chi(B)$ are $\mathcal{O}(1/\hbar)$ bigger than the corresponding terms in $m(B)$, and hence that the fluctuations will be significantly larger in this case.

3. The harmonic oscillator

The two-dimensional harmonic oscillator in a uniform magnetic field was extensively studied by Németh [17]. In this section we calculate $m_0(B)$ in the semiclassical limit, focusing in particular on its average behaviour.

The Hamiltonian is given by ($m = e = c = 1$)

$$H = \tfrac{1}{2}(p_x + By)^2 + \tfrac{1}{2}(p_y - Bx)^2 + \tfrac{1}{2}\varphi_1^2 x^2 + \tfrac{1}{2}\varphi_2^2 y^2 \tag{23}$$

and the energy levels by [17, 21]

$$E_{n_1 n_2} = \hbar\omega_1\left(n_1 + \tfrac{1}{2}\right) + \hbar\omega_2\left(n_2 + \tfrac{1}{2}\right) \tag{24}$$

where

$$\begin{aligned}\omega_1 &= \tfrac{1}{2}\left[\sqrt{B^2 + (\varphi_1 + \varphi_2)^2} + \sqrt{B^2 + (\varphi_1 - \varphi_2)^2}\right] \\ \omega_2 &= \tfrac{1}{2}\left[\sqrt{B^2 + (\varphi_1 + \varphi_2)^2} - \sqrt{B^2 + (\varphi_1 - \varphi_2)^2}\right].\end{aligned} \tag{25}$$

The exact result for m_0 is shown in figures 1 and 2 as a function of B and ω_1/ω_2 respectively, for $\hbar = 0.06$, $\varphi_1 = \sqrt{0.1}$, $\varphi_2 = \sqrt{2}$. It is clear from these figures that $m_0(B)$ shows an average increase in B and that it has peaks corresponding to values of B where the tori in phase space are resonant, i.e. filled with periodic orbits. Similar results have been obtained recently by Ullmo *et al* [22] for square billiards and, in a different context, in the magnetoresistence in lateral surface superlattices [23].

The average magnetization can be computed from the corrections to the leading-order (Weyl) approximation for the mean of the staircase function. Defining

$$Z(\beta) = \mathrm{tr}(\mathrm{e}^{-\beta H}) \tag{26}$$

it is obvious that $N(E)$ is the inverse Laplace transform of $Z(\beta)/\beta$. For the oscillator

$$Z(\beta) = \frac{1}{4\sinh(\beta\hbar\omega_1/2)\sinh(\beta\hbar\omega_2/2)} = \frac{1}{\hbar^2\beta^2\omega_1\omega_2}\left[1 - \frac{\hbar^2\beta^2}{4!}(\omega_1^2 + \omega_2^2) + \mathcal{O}(\hbar^4\beta^4)\right] \tag{27}$$

and hence we find that

$$\begin{aligned}\overline{N}(E) &= \frac{E^2}{2\hbar^2\omega_1\omega_2} - \frac{(\omega_1^2 + \omega_2^2)}{4!\omega_1\omega_2} \\ &= \frac{E^2}{2\hbar^2\varphi_1\varphi_2} - \frac{(B^2 + \varphi_1^2 + \varphi_2^2)}{4!\varphi_1\varphi_2}.\end{aligned} \tag{28}$$

Notice that this result is exact, since the terms in (27) which involve powers of β higher than the second give rise to contributions which are purely oscillatory.

As expected, the first (Weyl) term does not depend on B. Hence the only contribution to the average magnetization comes from the second term, which gives

$$\overline{m}_0(B) = \frac{BE_{\mathrm{f}}}{12P\varphi_1\varphi_2}. \tag{29}$$

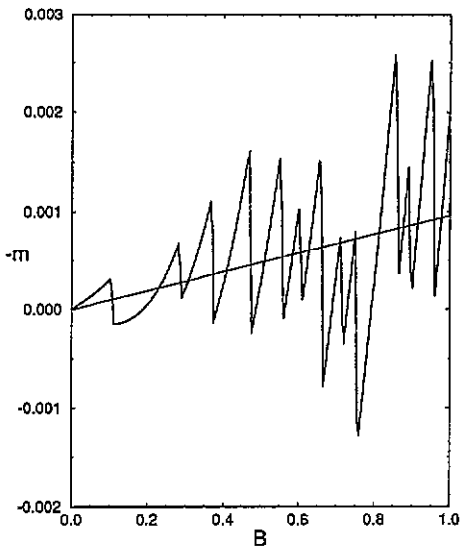

Figure 1. $-m_0$ as a function of B for the harmonic oscillator. The straight line indicates the average magnetization.

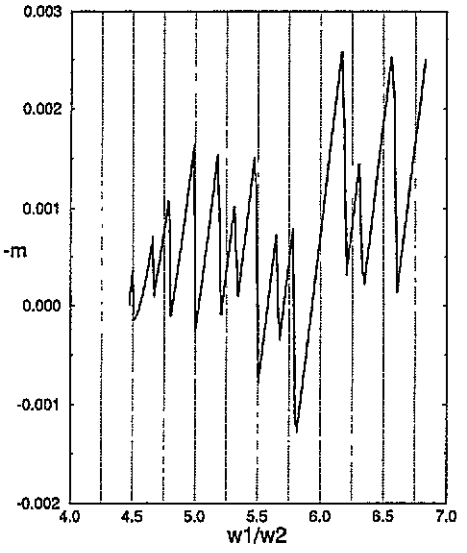

Figure 2. $-m_0$ as a function of w_1/w_2 for the harmonic oscillator with $P = 120$.

This straight line is shown in figure 1. It agrees very well with the numerical results.

4. A non-integrable model: chaos versus regularity

4.1. Single-particle features

The Hamiltonian now to be considered, sometimes called the 'Nelson Hamiltonian', is

$$H = \frac{1}{2m}(p_x + By)^2 + \frac{1}{2m}(p_y - Bx)^2 + (y - \tfrac{1}{2}x^2)^2 + 0.05x^2 \tag{30}$$

where we have again set $m = e = c = 1$. The motion which it generates can be shown to be bounded for all values of B and has been widely studied both classically, in terms of periodic orbits [24] and bifurcations [25], and quantum mechanically (for $B = 0$ only) [20, 26]. One of the advantages of working with a smooth system is that not only is it more realistic than the billiard systems previously studied [8, 10–12], but it is also non-integrable for all values of B, which makes it somewhat more generic.

In figures 3 and 4 we present sample Poincaré sections at relevant energies and values of B. For $B = 0$, chaotic motion sets in at about $E = 0.1$. For a fixed energy the character of the classical dynamics changes with the applied magnetic field, becoming more chaotic for moderate B (at a specific value which depends on the energy) and tending to regular for large B.

Of particular importance in our study is the behaviour of $\mathrm{d}S/\mathrm{d}B$ versus B for the periodic orbits (see (18) and (19)). We have computed this quantity for the principal orbits of the Nelson Hamiltonian and the results are shown in figure 9 for the case when $E = 0.314\,638$, which correspond to the Fermi energy for $P = 30$, $\hbar = 0.06$ and $B = 0$.

The eigenvalues of the Nelson Hamiltonian were computed by diagonalizing 700×700 complex Hermitian matrices in an appropriate basis [27]. To test their convergence we first compared these values with those obtained from a 1000×1000 diagonalization. This

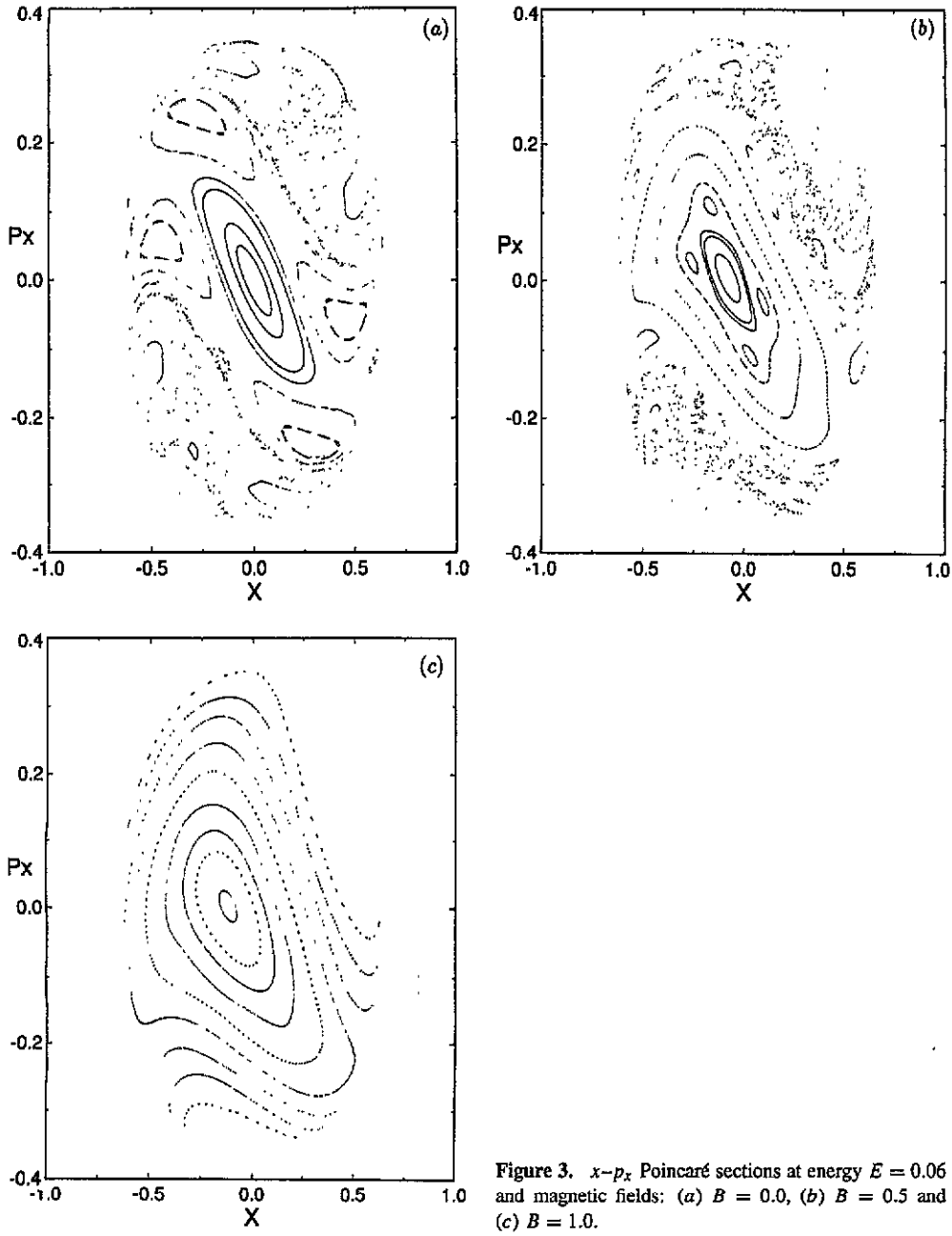

Figure 3. x–p_x Poincaré sections at energy $E = 0.06$ and magnetic fields: (*a*) $B = 0.0$, (*b*) $B = 0.5$ and (*c*) $B = 1.0$.

is, however, not sufficient to guarantee the quality of the results, because in order to evaluate derivatives with respect to the magnetic field we have to find the change in the E_n generated by very small changes in B. Therefore, we also compared the difference between the above diagonalizations at $B = 0$ (i.e. $E_n^{1000}(0) - E_n^{700}(0)$), with the difference $E_n^{700}(\Delta B) - E_n^{700}(0)$, where $\Delta B = 0.005$ is the field step-size used in our computations. Our subsequent calculations were performed using two values of $\hbar$, $\hbar = 0.06$ and $\hbar = 0.006$, for which an analysis of these energy-level differences showed that the number of converged

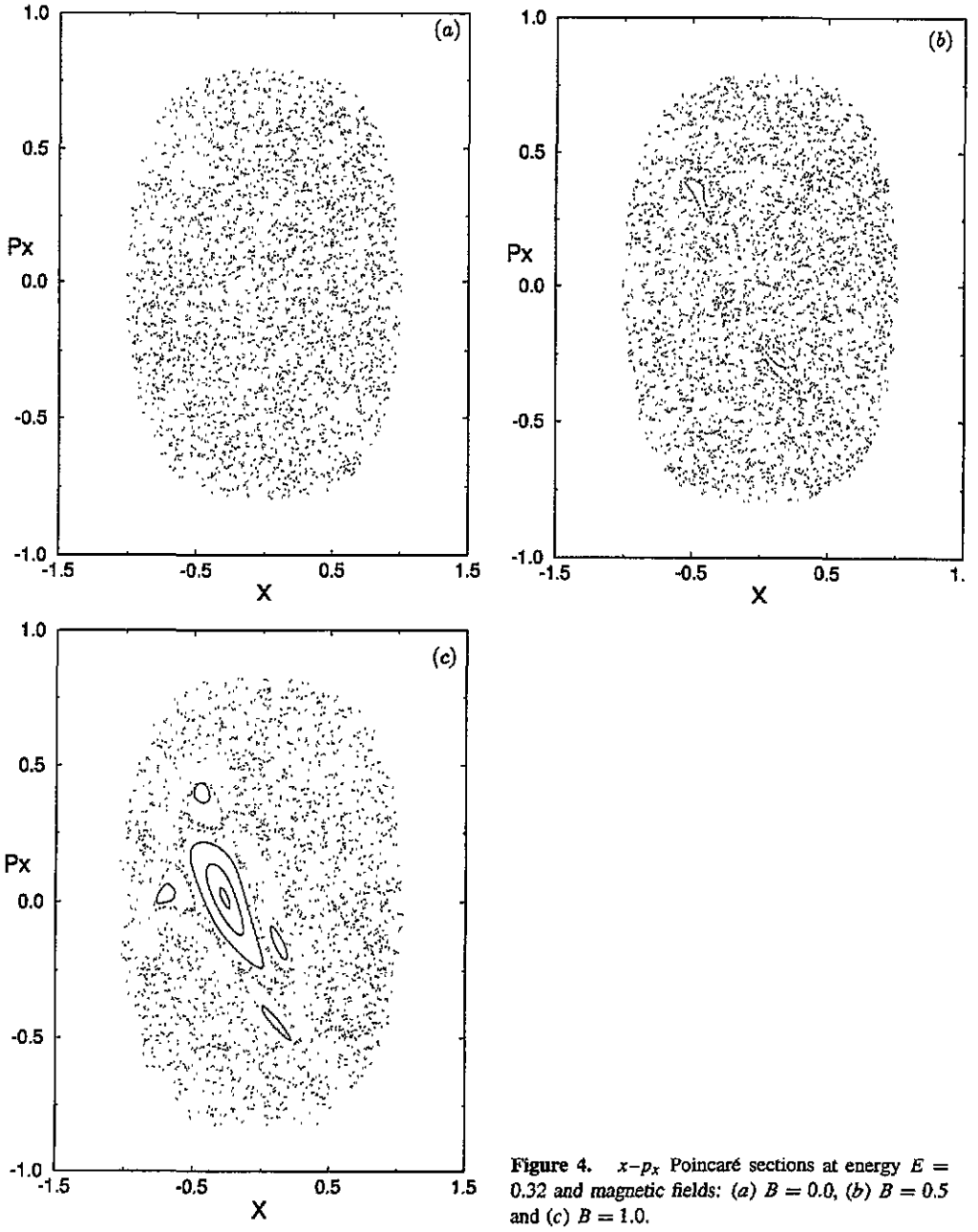

Figure 4. x–p_x Poincaré sections at energy $E = 0.32$ and magnetic fields: (*a*) $B = 0.0$, (*b*) $B = 0.5$ and (*c*) $B = 1.0$.

levels was about 30 in the first case and 150 in the second (although, for reasons to be explained below, we ultimately used only the first 120 of these in our calculations).

It follows that in the present study the two important ranges of energy are from zero to $E_r = 0.064\,303\,481$ and from zero to $E_c = 0.314\,638$, these values corresponding approximately to the 120th level for $\hbar = 0.006$ and the 30th level for $\hbar = 0.06$. The energy of the Poincaré sections in figure 3 corresponds to E_r. Clearly the orbits are still quite regular. For smaller energies we get increasingly regular plots; hence in the first energy

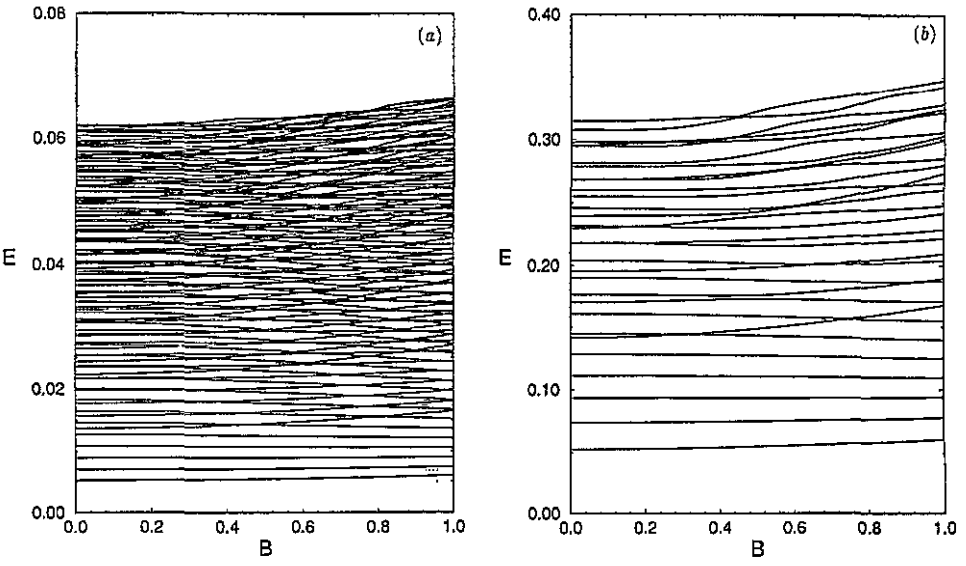

Figure 5. Dependence of the energy levels on the scaled field B. (a) shows the first 120 'regular') levels for $\hbar = 0.006$; (b) shows the first 30 ('chaotic') levels for $\hbar = 0.06$ ('chaotic levels').

range the classical motion is almost entirely integrable. By contrast, it may be seen from figure 4 that the second range is mostly chaotic for $B \in [0, 1]$, in the sense that the regular portion of the phase space is a very small fraction of the total.

Figures 5(a) and (b) show the dependence of the energy levels on the scaled field B. The spectra were computed for 200 values of B in the interval $(0, 1)$ at constant step $\Delta B = 0.005$. When $\hbar = 0.006$ the first 120 states are regular, while for $\hbar = 0.06$ most of the first 30 lie in the chaotic range (only the first three are still in the regular region). Henceforth, these two cases will simply be referred to as 'regular' and 'chaotic', respectively.

4.2. Magnetization and periodic orbits.

We computed the magnetization per particle at zero temperature (equation (3)) for both the regular and chaotic spectra. The results for the regular case (figure 6(a)) are very similar to those of section 3 for the harmonic oscillator, with the periodic tori playing the most important role. The chaotic case (figure 6(b)) is, however, strikingly different, and we now analyse these results in terms of the semiclassical theory developed in section 2.

The first terms in the asymptotic expansion of the average of the staircase function for the Nelson Hamiltonian can be computed directly. An outline of the calculation is presented in the appendix; the result is identical to the expression for the harmonic oscillator (28) with $\varphi_1 = \sqrt{0.1}$ and $\varphi_2 = \sqrt{2}$. Hence, once again, the Weyl term itself does not influence the magnetization: the main contribution comes from the correction terms and leads to an average linear increase given by (29).

Figures 6(a) and (b) display the numerically computed $m_0(B)$. It should be stressed that in this case equation (29) is expected to represent a good approximation for $\overline{m}_0(B)$ only for small fields B; further (nonlinear) contributions, not present for the harmonic oscillator, may be derived from neglected higher-order terms in the full Weyl expansion for $\overline{N}$. It is,

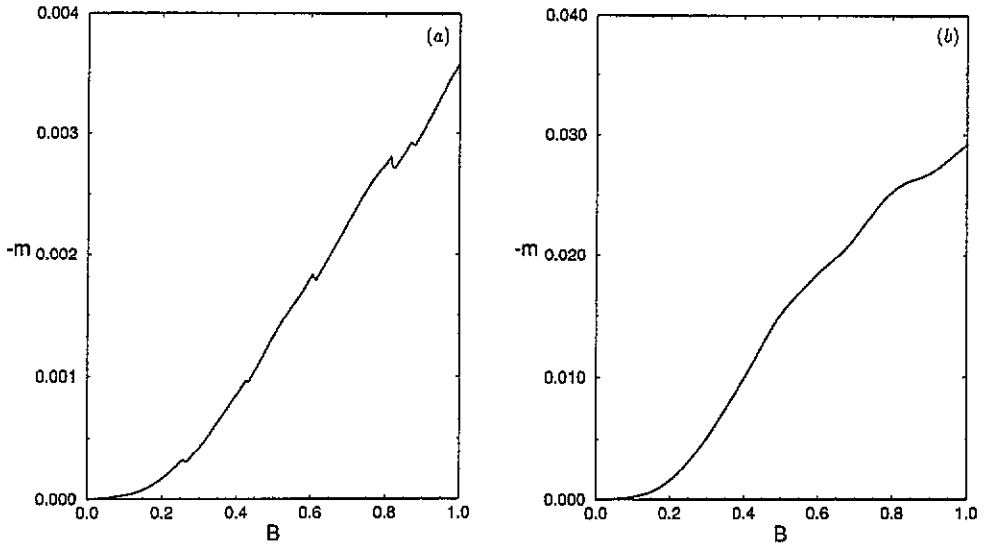

Figure 6. $-m_0$ as a function of B. (a) shows the result for the regular levels and (b) shows the result for the chaotic levels.

of course, also the case that the gradient of $m_0(B)$ at $B = 0$, that is, $\chi_0(0)$, fluctuates around the mean as the number P of electrons changes. Therefore, a plot of $\chi_0(0)$ as a function of P represents a more complete test. The expectation for the average behaviour is that

$$\overline{\chi}_0(0) = \frac{E_f(0)}{12P\varphi_1\varphi_2} = \frac{\hbar}{12\sqrt{\varphi_1\varphi_2 P}} \tag{31}$$

where we have used (28) to write E_f as a function of P. This follows because the average with respect to P obviously corresponds to an average over E_f and hence has the effect of removing the periodic orbit contributions. It is shown, together with the numerically computed values, in figures 7(a) and (b) for the regular and chaotic cases, respectively. The results confirm that our computations are reliable for P up to 30 if $\hbar = 0.06$ and for P up to about 120 for $\hbar = 0.006$ (rather than 150 as suggested by the tests described in the previous subsection).

Equation (31) is most interesting when viewed in the light of the conjecture by Nakamura and Thomas [8] that the size of $\chi_0(0)$ should reflect the chaotic nature of the underlying classical mechanics. The theory outlined above suggests the opposite, namely that when averaged over P, $\chi_0(0)$ will in fact depend only on general features of the system in question, features which are not related to orbit stability. Specifically, the average of $\chi_0(0)$ is independent of the precise nature of the dynamics in the same way that (and in fact because) the first terms in Weyl's asymptotic expansion of the mean staircase are. The numerical results described above confirm this for the Nelson Hamiltonian.

Exactly the same conclusion also follows for Aharanov–Bohm billiards [28], since for these systems it is also known that the first two terms of the Weyl series (i.e. the area and perimeter contributions) are independent of B, but the third (i.e. the 'constant') is given by

$$C(\phi) = C(0) - \phi(1-\phi)/2 \tag{32}$$

where $C(0) = \frac{1}{6}$ for any billiard with a smooth boundary, and ϕ is the (quantum) magnetic flux taken modulo 1 [29]. Hence this term also gives rise to a net mean magnetization

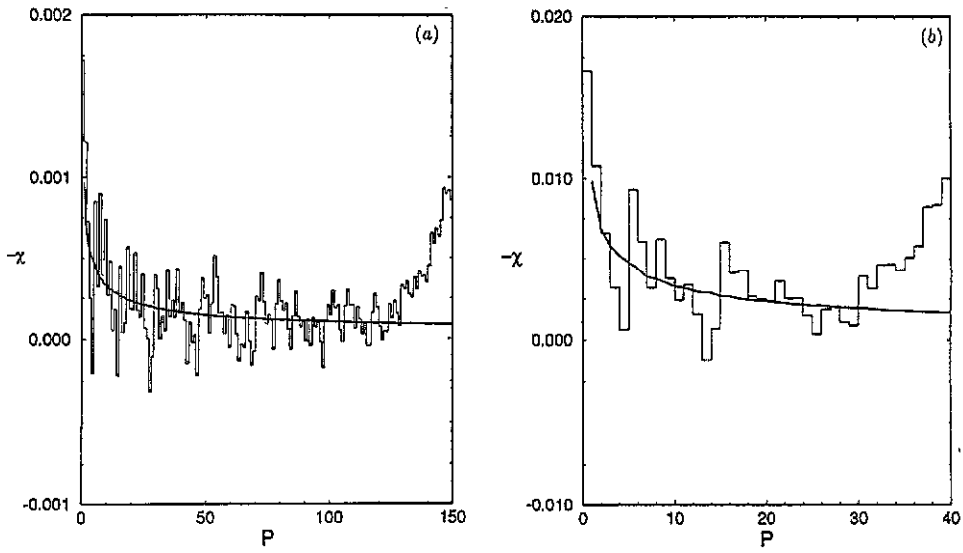

Figure 7. $-\chi_0$ as a function of P for (a) the regular levels, $1 \leqslant P \leqslant 150$, and ($b$) the chaotic levels, $1 \leqslant P \leqslant 50$. The curve represents the theoretical result (31).

which is independent of whether the billiard supports integrable, mixed, or chaotic classical motion when averaged with respect to the number of electrons.

It follows from the analysis of section 2 that the chaotic nature of the associated classical flow is expected to show itself in the fluctuations of the magnetization about its mean. These are most easily studied by taking the Fourier transform of $m_0^{\rm osc}(B)$. Numerically, we obtained this oscillatory part by subtracting from m_0 its average, computed directly rather than simply using (29) since, for the reasons noted above, the analytical approximation is only valid for small values of B.

In figure 8 we show this Fourier transform and compare the peaks with the values of $\mathrm{d}S/\mathrm{d}B$ for the shortest periodic orbits. Although the plot indicates that the most pronounced peak indeed corresponds to the first orbit, it is difficult to take this analysis further, because each orbit in fact contributes more than once (see equation (20)). Therefore, a better test of our semiclassical theory is provided by considering the local Fourier transform over a range ΔB, defined as

$$\tilde{m}_T^{\rm osc}(a, B, \Delta B) = \int_{-\infty}^{+\infty} m_T^{\rm osc}(B + x)\mathrm{e}^{-\mathrm{i}ax/\hbar}\mathrm{e}^{-x^2/(2\Delta B^2)}\,\mathrm{d}x\,. \tag{33}$$

Using (17) for $m_T^{\rm osc}$ and assuming $\Delta B \ll B$, we have that semiclassically

$$\tilde{m}_T^{\rm osc}(a, B, \Delta B) \approx \frac{2KT}{\hbar P}\sum_P\sum_{j=1}^{\infty} A_{p,j}a_p\frac{\mathrm{e}^{-\pi KT\tau_{p,j}/\hbar}}{1-\mathrm{e}^{-2\pi KT\tau_{p,j}/\hbar}}I(a, B, \Delta B) \tag{34}$$

where the function

$$I(a, B, \Delta B) = \frac{\sqrt{2\pi}\Delta B}{2\mathrm{i}} \times\left[\mathrm{e}^{ij(S_p/\hbar-\pi\sigma_p/2)}\mathrm{e}^{-(a-ja_p(B))^2\Delta B^2/2\hbar^2} - \mathrm{e}^{-ij(S_p/\hbar-\pi\sigma_p/2)}\mathrm{e}^{-(a+ja_p(B))^2\Delta B^2/2\hbar^2}\right]$$

has Gaussian peaks at $a = \pm ja_p(B)$. This then has the effect of selecting from the i-sum in (20) the particular contribution with $B_i \approx B$.

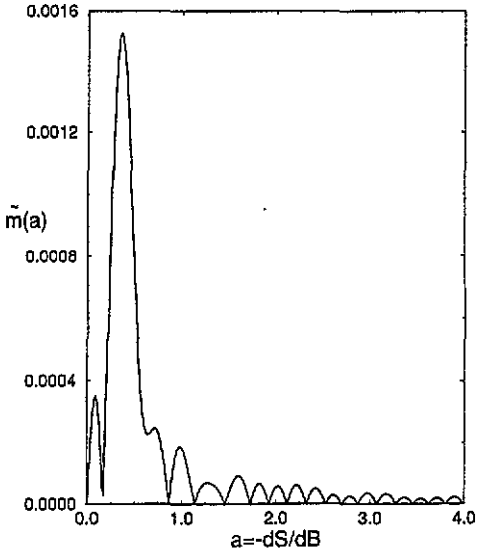

Figure 8. Fourier transform of $m_0^{osc}(B)$ for the chaotic case.

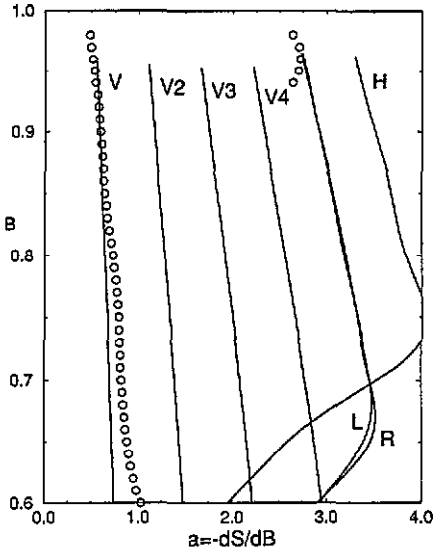

Figure 9. Magnetic field versus position of the maxima in the local Fourier transform. The full lines represent the shortest periodic orbits at energy $E = 0.314638$. The labelling follows the notation of [25].

We performed a numerical computation of (33) with $T = 0$. For each value of B a local Fourier transform was calculated and the position $a(B)$ of the largest peak tabulated. Figure 9 shows the resulting plot of B versus $a(B)$ superimposed on the corresponding curves for the periodic orbits. It confirms very clearly the strong influence of the shortest orbit on m_0^{osc}. Interestingly, it follows from the Poincaré sections presented earlier that this orbit is, in fact, stable when $B \approx 1$, which probably accounts for the dominance of its contribution. They show as well that the V4 orbit also becomes stable at this field value, explaining its appearance in the figure too. Obviously we would like to be able to go further and identify the contributions from other orbits in the same way; unfortunately, given the data currently at our disposal (i.e. using only 30 levels) this has not proved possible.

4.3. Fluctuations in the susceptibility and size effects

Having computed the magnetization, it is simple to calculate the susceptibility

$$\chi(B) = \frac{\partial m}{\partial B} \tag{35}$$

for the regular and chaotic regimes. The results, displayed in figures 10(a) and (b), show that the nature of the classical dynamics also has a strong influence on $\chi(B)$. Indeed, the difference between the two regimes is much more evident here than in $m(B)$ since, as discussed in section 2, the fluctuations are stronger. It is interesting to note that the peaks associated with avoided crossings are particularly sharp in the first (regular) case; the fact that they all correspond to enhanced susceptibility directly supports the explanation of this phenomenon given in the introduction.

The dependence of χ on the system size, or number P of electrons, is shown in figures 11(a) and (b) for three different values of the magnetic field. From these plots we conclude that in both the regular and chaotic cases χ fluctuates with P, the average amplitude of these

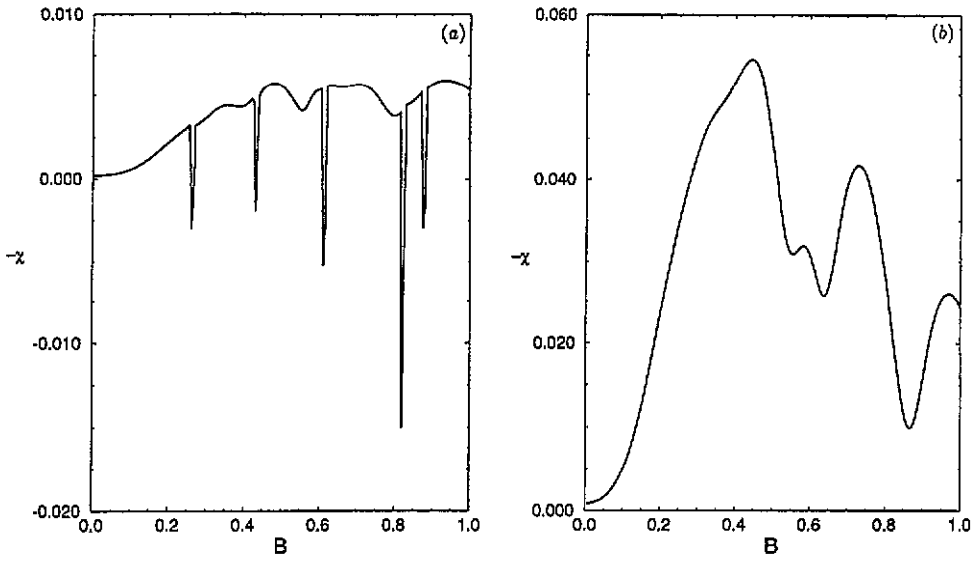

Figure 10. $-\chi_0$ as a function of B: (a) shows the result for the regular levels and (b) the result for the chaotic levels.

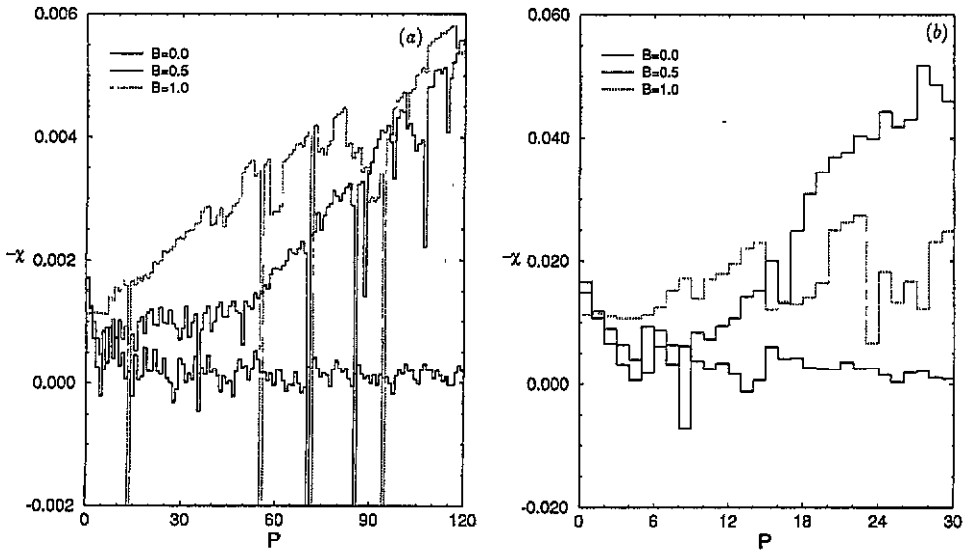

Figure 11. $-\chi_B$ as a function of P for $B = 0$, 0.05 and 1.0: (a) regular levels, $1 \leqslant P \leqslant 120$, and ($b$) chaotic levels, $1 \leqslant P \leqslant 30$.

fluctuations being about twice as large in the chaotic regime (modulo an additional factor of 10 due to the different values of $\hbar$ involved). One important difference is the presence of anomalous fluctuations in the regular regime. These can again be readily identified as avoided crossings at the corresponding values of P and B (see figure 6(a)). Notice that this effect is most pronounced when $B = 1.0$, which represents the most regular case. Except for these anomalies, the amplitude of the fluctuations decreases as B increases.

5. Conclusions

We have studied the semiclassical behaviour of the magnetization in a two-dimensional non-interacting electron gas both theoretically, in the semiclassical limit, and numerically. It has been shown that the fluctuational properties of $m(B)$ depend strongly on the chaotic nature of the underlying classical dynamics. As is usual in semiclassical theories, the periodic orbits play a distinctive role in their description. Moreover, although there is no contribution from the Weyl term itself (no classical diamagnetism), there is a net average magnetization arising from (quantum) corrections to the mean staircase, that is, from later terms in the Weyl expansion. Interestingly, this average is independent of the stability of the classical orbits. This implies that when the zero-field susceptibility is averaged with respect to the system size (i.e. with respect to the number P of electrons) it too should turn out to be similarly independent. This would then appear to contradict the Nakamura–Thomas conjecture, at least in the average sense. The numerical results presented here (for $T = 0$ only) confirm these semiclassical predictions.

Acknowledgments

This paper was partly supported by CNPq, Fapesp and Finep. JPK is grateful to CNPq and to the Royal Society for financing a visit to Brazil during which his part of this collaboration took place. He also wishes to acknowledge the Physics department at UNICAMP and in particular Professor A M Ozorio de Almeida for the generous hospitality enjoyed during this period.

Appendix.

In this appendix we outline the derivation of the partition function for the Nelson Hamiltonian (equation (30)). Our method is essentially the same as that described in more detail in [30].

The partition function is given by

$$Z(\beta) = \mathrm{tr}\left(\mathrm{e}^{-\beta\hat{H}}\right) = \frac{1}{(2\pi\hbar^2)}\int \mathrm{d}q^2\,\mathrm{d}p^2\left[\mathrm{e}^{-\beta\hat{H}}\right]_{\mathrm{W}}$$

where

$$\left[\mathrm{e}^{-\beta\hat{H}}\right]_{\mathrm{W}} \equiv U_{\mathrm{W}} = \int \mathrm{d}y^2\left\langle q + \tfrac{1}{2}y\right|\mathrm{e}^{-\beta\hat{H}}\left|q - \tfrac{1}{2}y\right\rangle \mathrm{e}^{-\mathrm{i}py/\hbar}$$

is the Weyl transform of the operator $\mathrm{e}^{-\beta\hat{H}}$. Using the operator product formula [30], we may write

$$\left[\hat{H}\mathrm{e}^{-\beta\hat{H}}\right]_{\mathrm{W}} = -\frac{\partial U_{\mathrm{W}}}{\partial\beta} = H_{\mathrm{W}}\cos\left(\frac{\hbar\overleftrightarrow{\Lambda}}{2}\right)U_{\mathrm{W}}$$

where

$$\overleftrightarrow{\Lambda} = \overleftarrow{\nabla}_q\overrightarrow{\nabla}_p - \overleftarrow{\nabla}_p\overrightarrow{\nabla}_q\,.$$

The above expression can be expanded as power series in $\hbar$:

$$-\frac{\partial U_{\mathrm{W}}}{\partial\beta} = H_{\mathrm{W}}U_{\mathrm{W}} - \tfrac{1}{8}\hbar^2 H_{\mathrm{W}}\overleftrightarrow{\nabla}^2 U_{\mathrm{W}} + \mathcal{O}(\hbar^4)\,.$$

In zeroth order we get $U_W = e^{-\beta H_W}$. Writing

$$U_W = e^{-\beta H_W}\left[1 - \tfrac{1}{8}\hbar^2 A_1 + \mathcal{O}(\hbar^4)\right]$$

we then find an equation for A_1,

$$-\frac{\partial A_1}{\partial \beta} = e^{\beta H_W}\left[H_W \overleftrightarrow{\Lambda}^2 e^{\beta H_W}\right]$$

in terms of which

$$Z(\beta) = \frac{1}{(2\pi\hbar^2)}\int dp^2\, dq^2\, e^{-\beta H_W}\left[1 - \tfrac{1}{8}\hbar^2 A_1 + \mathcal{O}(\hbar^4)\right].$$

Solving for A_1 using the Nelson Hamiltonian, we find that

$$Z(\beta) = \frac{1}{\hbar^2\beta^2\varphi_1\varphi_2}\left[1 - \frac{\hbar^2\beta^2}{4!}(\beta^2 + \varphi_1^2 + \varphi_2^2) + \mathcal{O}(\hbar^4)\right]$$

where $\varphi_1 = \sqrt{0.1}$ and $\varphi_2 = \sqrt{2}$. Taking the inverse Laplace transform of $Z(\beta)/\beta$ yields equation (28) plus corrections of order $\hbar^4$.

References

[1] Gutzwiller M C 1990 *Chaos in Classical and Quantum Mechanics* (New York: Springer)
[2] Ozorio de Almeida A M 1988 *Hamiltonian Systems: Chaos and Quantization* (Cambridge: Cambridge University Press)
[3] Berry M V 1991 *Chaos and Quantum Physics (Les Houches Lecture Series 52)* ed M-J Gianoni, A Voros and J Zinn-Justin (Amsterdam: North-Holland)
[4] Delande D 1991 *Chaos and Quantum Physics (Les Houches Lecture Series 52)* ed M-J Gianoni, A Voros and J Zinn-Justin (Amsterdam: North-Holland)
[5] Wintgen D 1988 *Phys. Rev. Lett.* **61** 1803
[6] Main J, Wienbusch G, Welge K, Shaw J and Delos J B 1994 *Phys. Rev.* A (to appear)
[7] Meyer K R, Delos J B and Mao J-M 1992 *Proc. Conservative Systems and Quantum Chaos Workshop (Waterloo)* ed D Rod
[8] Nakamura K and Thomas H 1988 *Phys. Rev. Lett.* **61** 247
[9] Bohigas O 1991 *Chaos and Quantum Physics (Les Houches Lecture Series 52)* ed M-J Gianoni, A Voros and J Zinn-Justin (Amsterdam: North-Holland)
[10] Robnik M and Berry M V 1985 *J. Phys. A: Math. Gen.* **18** 1361
[11] Traiber A J S, Fendrik A J and Bernath M 1990 *J. Phys. A: Math. Gen.* **23** L305
[12] Berman D, Entin-Wohlman Ora and Azbel M Ya 1990 *Phys. Rev.* B **42** 9299
[13] Gutzwiller M C 1971 *J. Math. Phys.* **12** 343
[14] Oded Agam 1993 The magnetic response of chaotic mesoscopic systems *Preprint* TECHNION-PHY-93
[15] Keating J P 1992 *Proc. R. Soc.* A **436** 99–108
[16] Berry M V and Keating J P 1992 *Proc. R. Soc.* A **437** 151–73
[17] Németh R 1990 Z. *Phys.* B **81** 89
[18] Huang K 1963 *Statistical Mechanics* (New York: Wiley)
[19] Peierls R E 1955 *Quantum Theory of Solids* (Oxford: Oxford University Press) pp 144–6
[20] Malta C P, de Aguiar M A M and Ozorio de Almeida A M 1993 *Phys. Rev.* A **47** 1625
[21] Schuh B 1985 *J. Phys. A: Math. Gen.* **18** 803
[22] Ullmo D, Richter K and Jalabert R A 1993 *Preprint* IPNO/TH 93-60
[23] Fleischmann R, Geisel T and Ketzmerick R 1992 *Phys. Rev. Lett.* **68** 1367
[24] Baranger M, Davies K T R and Mahoney J H 1988 *Ann. Phys., NY* **186** 95
[25] Prado S D and de Aguiar M A M 1994 *Ann. Phys., NY* (at press)
[26] Provost D and Baranger M 1993 *Phys. Rev. Lett.* **71** 66
[27] Provost D 1992 *PhD thesis* (Cambridge, MA: MIT)
[28] Berry M V and Robnik M 1986 *J. Phys. A: Math. Gen.* **19** 649–68
[29] Berry M V 1986 *J. Phys. A: Math. Gen.* **19** 2281–96
[30] Hillery M *et al* 1984 *Phys. Rep.* **106** 121